Influence of Macromolecular Architecture on the Thermal Response Rate of Amphiphilic Copolymers, Based on Poly(*N*-isopropylacrylamide) and Poly(oxyethylene), in Water

Kurt Van Durme,[†] Guy Van Assche,[†] Vladimir Aseyev,[‡] Janne Raula,[§] Heikki Tenhu,[‡] and Bruno Van Mele*,[†]

Department of Physical Chemistry and Polymer Science, Vrije Universiteit Brussel, Brussels, Belgium; Laboratory of Polymer Chemistry, University of Helsinki, Helsinki, Finland; and NanoMaterials Group, Center for New Materials and Laboratory of Physics, Helsinki University of Technology, Helsinki, Finland

Received November 3, 2006; Revised Manuscript Received March 4, 2007

ABSTRACT: The effect of poly(oxyethylene), PEO, on the thermal response rate of aqueous solutions of poly(*N*-isopropylacrylamide), PNIPAM, block and graft copolymers has been discussed. The PNIPAM-*b*-PEO/water system reveals thermoresponsive properties similar to the PNIPAM/water system. In PNIPAM-*g*-PEO/water solutions, however, PEO provides hydrophilic channels, facilitating the diffusion of water molecules through the collapsed polymer aggregate at temperatures above the demixing temperature of the aqueous copolymer solution. As a result, the thermal response of the aqueous PNIPAM-*g*-PEO system is significantly faster than in the case of either pure PNIPAM or PNIPAM-*b*-PEO, indicating the influence of the macromolecular architecture. An attempt has also been made to correlate the thermal response kinetics of the aqueous solutions of different copolymers with the miscibility of the polymer constituents, i.e., PEO and the thermoresponsive PNIPAM backbone, which can vitrify during phase separation.

Introduction

Thermoresponsive aqueous polymer systems are known to exhibit large, reversible conformational changes in response to small thermal stimuli.[1] These aqueous polymer systems are often characterized by a lower critical solution temperature (LCST) type of miscibility behavior, which implies that the polymer dissolves in water at low temperature and phase separates upon heating. Moreover, thermoresponsive homo- and copolymers are known to collapse when phase separation sets in. As a result, at low polymer concentration colloidally stable suspensions can be attained,[2] whereas the cross-linked analogues (i.e., hydrogels) show an order-of-magnitude shrinking.[3−8] Therefore, thermosensitive polymeric materials, often called intelligent, can be used as actuators,[9,10] artificial muscles,[11] dewatering membranes,[12] drug delivery systems,[13−16] thermoresponsive surfaces,[17−19] light modulation systems,[20,21] and molecular recognition agents.[22,23]

Poly(*N*-isopropylacrylamide) (PNIPAM) is probably the most studied thermosensitive polymer,[24,25] especially in dilute solutions.[26−29] At low temperatures, intermolecular hydrogen bonds between water and polar groups of PNIPAM solubilize the polymer.[30−33] Above the demixing temperature (T_{demix}), hydrogen bonds break and hydrophobic associations between the collapsed polymer chains take place, which is accompanied by rising opacity and an endothermic heat effect.[8,30,34−37] Recently, it was demonstrated that the PNIPAM-rich phase, formed above T_{demix}, vitrifies upon further heating due to the interference of the LCST type of demixing curve with the glass transition temperature (T_g) vs composition curve.[8,36,37] It has also been suggested that macroscopic phase separation might be arrested by partial vitrification of the polymer-rich phase when a solution of low PNIPAM concentration is quickly heated well above T_{demix}.[2] However, additional experimental confirmation is needed to clarify this issue.

The occurring partial vitrification slows down the subsequent remixing (reswelling) upon cooling,[8,36−38] which is a major drawback regarding the potential applicability of this system since usually a fast change from heterogeneous to homogeneous and vice versa is required. Therefore, the improvement of the thermal response rate of PNIPAM-based materials has been extensively investigated during the past couple of years.[39] One possibility to increase the remixing (or reswelling) rate is to introduce hydrophilic poly(oxyethylene) (PEO) grafts, which enhance the diffusion of water molecules inside the collapsed, vitrified polymer-rich phase.[40,41] These PEO chains seem to provide hydrophilic channels,[40] facilitating the diffusion of water molecules throughout the polymer matrix. Additionally, the macromolecular architecture might also influence the thermoresponsive behavior, as it affects the dimension, spatial distribution, and the number of PEO channels within the PNIPAM-rich phase. In this report, aqueous solutions of PNIPAM-based block and graft copolymers have been compared, and the thermal response rate of the copolymers is discussed. Moreover, an attempt has been made to correlate the modified kinetics of the aqueous copolymer system with the miscibility of the copolymer constituents, i.e., PEO and PNIPAM. The blend miscibility of PNIPAM and PEO with varying molar mass of PEO has been studied using modulated temperature differential scanning calorimetry (MTDSC), which has already proven to be a powerful tool for characterizing binary polymer systems.[8,36,41−43]

Experimental Section

Materials. Copolymers of poly(*N*-isopropylacrylamide) (PNIPAM) with either poly(oxyethylene) (PEO) blocks or grafts were synthe-

[†] Vrije Universiteit Brussel.
[‡] University of Helsinki.
[§] Helsinki University of Technology.
* Corresponding author: Fax +32-(0)2-6293278; Ph +32-(0)2-6293288; e-mail bvmele@vub.ac.be.

10.1021/ma062538g CCC: $37.00
Published on Web 04/19/2007

Table 1. Molecular Characteristics of the (Co)polymers Studied

(co)polymer	molar mass (g mol^{-1}) PNIPAM	PEO	
PNIPAM	187 000[a]		
PNIPAM-*g*-PEO	180 000[b]	6000[c]	6 grafts/backbone
	180 000[b]	6000[c]	10 grafts/backbone
PNIPAM-*b*-PEO	39 000[d]	550[e]	diblocks
	151 000[d]	550[e]	diblocks
	345 000[d]	550[e]	diblocks

[a] Determined using the Mark−Houwink equation $[\eta] = KM_v^a$, with $K = 0.0299$ mL g^{-1} and $a = 0.64$ at 25 °C. [b] Determined for PNIPAM-*co*-GMA in THF using static light scattering. [c] Provided by Shearwater Polymers. [d] Determined in $CDCl_3$ using NMR. [e] Provided by Fluka.

sized according a procedure reported earlier.[44,45] In short, graft-copolymers were prepared by postgrafting of a statistical copolymer of PNIPAM and glycidyl methacrylate (GMA), whereas the block copolymers were synthesized by polymerization of NIPAM monomer using preformed PEO macroazoinitiators. Their molecular characteristics are given in Table 1. In the case of graft-copolymers, the weight-average molar mass (M_w) of the functionalized PNIPAM-*co*-GMA backbone was determined using static light scattering. From NMR one gets the ratio of NIPAM and EO units, which enables calculating the total molar mass of the copolymers. In the case of block copolymers, the molar masses and NIPAM/EO ratio were obtained directly from NMR.

Molar mass distributions were taken from SEC. For PNIPAM-*co*-GMA (in the case of graft-copolymers) the polydispersity index equals 3.4.[46] This somewhat high value results from the free radical polymerization and from the known difficulties to characterize PNIPAM by SEC.[47] For the block copolymers the polydispersity was 1.5−1.6. However, in frames of the presented research polydispersity of PNIPAM has minor influence on the phase separation behavior.

PNIPAM homopolymer (reference material) was obtained from Polymer Source (viscosity average molar mass, $M_v = 187\,000$ g mol^{-1}, polydispersity index 2.6) and dried under vacuum for at least 48 h at 150 °C prior to use. The T_g of dried PNIPAM is ca. 140 °C, as measured by MTDSC. PEO homopolymers were purchased from VWR international ($M_w = 300$ g mol^{-1}, $T_g = -78$ °C) and Acros Organics ($M_w = 1000$ g mol^{-1}, $T_g = -67$ °C). Deionized water was used to prepare all aqueous solutions.

Sample Preparation. Aqueous polymer solutions with concentrations spanning the entire composition range were prepared directly in aluminum DSC crucibles (Mettler) that can be sealed hermetically. All samples were made starting from a 10/90 (w/w) polymer/water stock solution that was prepared by adding water to the dried polymer. DSC pans with solutions containing more than 10 wt % of polymer were obtained by evaporation of water (at room temperature), while those containing less than 10 wt % of polymer were obtained by dilution of the original 10/90 solution. Once the desired composition was attained, the crucibles were hermetically sealed and stored at 4 °C (for at least a month) to obtain a homogeneous solution.

Polymer blends of PNIPAM and PEO were prepared by solution casting. Different blend compositions were obtained by mixing the appropriate amounts (w/w) of the dried polymers with a common solvent (chloroform). These ternary mixtures were continuously stirred for at least 1 week in order to ensure homogeneity. After that they were put in a vacuum oven at 45 °C to evaporate the solvent. Thermogravimetric analysis (TGA) was used to check the preparation procedure, showing that each polymer blend contained less than 1 wt % residual solvent.

Experimental Methods. Modulated temperature differential scanning calorimetry (MTDSC) measurements were performed on a TA Instruments Q1000 (T-zero DSC-technology) with either a refrigerated (RCS) or liquid nitrogen (LNCS) cooling system. Helium (for RCS) or nitrogen (for LNCS) was used as a purge gas (25 mL min^{-1}). Indium and cyclohexane were used for temperature calibration. The former was also used for enthalpy calibration. Standard modulation conditions were an amplitude of 0.50 °C and a period of 60 s. Heat capacity calibration was performed under standard modulation conditions with water using the heat capacity difference between two temperatures, one above and one below the melting temperature. This way, the most accurate measurements of the heat capacity changes and "excess" contributions, c_p^{excess}, were obtained. Data were expressed as specific heat capacities (or changes) in J g^{-1} K^{-1}. Note that when studying phase separation and the associated kinetics, the variation of the specific heat capacity as a function of both temperature and time is more relevant than its absolute value. Nonisothermal experiments were performed at an underlying heating/cooling rate of 0.2 or 1 °C min^{-1}.

Results and Discussion

A. Aqueous (Co)polymer Solutions. 1. Nonisothermal Demixing/(Re)mixing of Aqueous Polymer Solutions: State Diagram. Before evaluating the effect of the macromolecular architecture on the phase behavior of thermoresponsive PNIPAM-based copolymers containing PEO, the phase behavior of the binary PNIPAM/water system is described briefly. A more detailed MTDSC analysis was previously published.[8,36,37] When heating a homogeneous aqueous PNIPAM solution, phase separation occurs as a result of changing polymer hydration, which can be observed as an endothermic heat effect.[30−33] By means of MTDSC, the total demixing enthalpy is separated in two endothermic contributions; the largest part (usually more than 90%) is found in the reversing heat flow signal (which is proportional to the heat capacity signal derived from the modulated heat flow), whereas the nonreversing heat flow contains the remaining fraction. A complete description of the extraction of the heat capacity and other MTDSC signals can be found in the literature.[48−50] Since part of the heat effect is found in the specific heat capacity signal, the latter is termed apparent (c_p^{app}) to distinguish it from the baseline specific heat capacity (c_p^{base}). It is worth noting that the endothermicity found in the excess heat capacity signal ($c_p^{excess} = c_p^{app} - c_p^{base}$) originates from demixing/remixing processes at the polymer/water interphase of the coexisting phases, which are fast on the time scale of the modulation, as has been thoroughly elaborated in previous work.[36,43]

The upper curves in Figure 1a illustrate the evolution of c_p^{app} with temperature for a 20/80 $PNIPAM_{187000}$/water solution. The initial deviation of c_p^{app} (thick line) from the extrapolated experimental baseline heat capacity, c_p^{base} (dashed line), defines the start of phase separation. Hence, by using a threshold value against c_p^{base}, the demixing temperature (T_{demix}, indicated by the dashed arrow in Figure 1a) was obtained.[36] If the demixed aqueous polymer solution is heated beyond the intersection of the LCST type of demixing curve with the T_g−composition curve (indicated by the oval in Figure 1b), the PNIPAM-rich phase formed will (partially) vitrify, as its T_g is close to the experimental temperature.[8,36,37] A partially vitrified PNIPAM-rich phase is a phase for which the temperature is within its (gradually increasing) glass transition interval, leading to a behavior that is between liquid and glassy. Since (partial) vitrification generates diffusion restrictions, the phase separation process slows down and a smaller c_p^{excess} is observed. In addition, it results in a heat capacity decrease for the PNIPAM-rich phase (smaller c_p^{base}).

The occurrence of (partial) vitrification of the PNIPAM-rich phase during phase separation was demonstrated by heating a more concentrated (70/30) $PNIPAM_{187000}$/water solution up to 60 °C (not shown), followed by a quench-cooling (using liquid nitrogen) to freeze in the formed phases. In the subsequent heating a glass transition temperature was seen at 32 °C (ranging

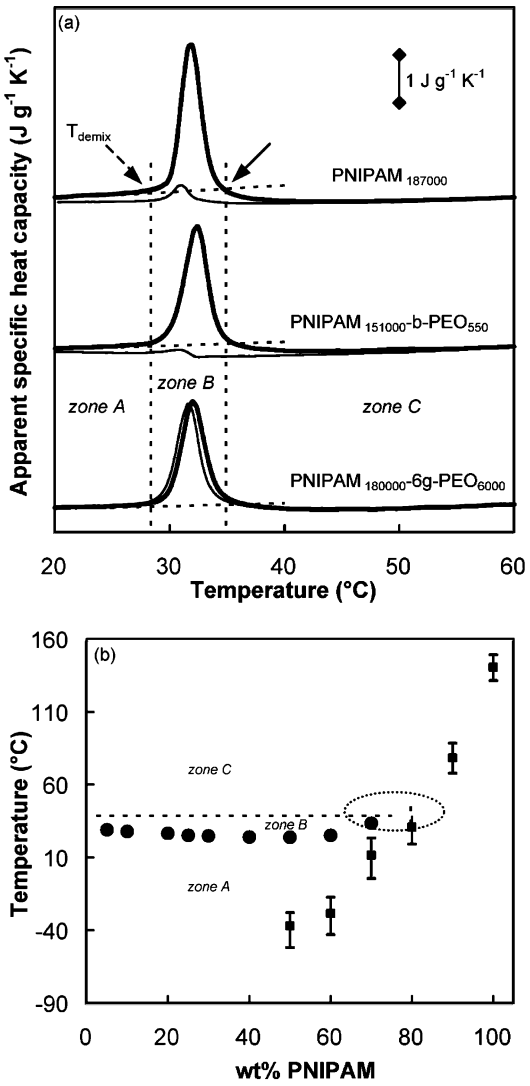

Figure 1. (a) c_p^{app} during nonisothermal demixing (heating: thick lines) and remixing (cooling: thin lines) of a 20/80 polymer/water solution. Dashed line (extrapolated experimental c_p^{base}) is a guide to the eye. Vertical (dashed) lines indicate T_{demix} (zone A → zone B) and drop of c_p^{app} below c_p^{base} (considered as onset of partial vitrification, zone B → zone C). Curves are shifted vertically for clarity. (b) State diagram for $PNIPAM_{187000}$/water with LCST type of demixing curve (●), T_g−composition curve of homogeneous solutions (■) with vertical bars indicating the width of the glass transition, and (dashed) line indicating the onset of partial vitrification. A homogeneous region (zone A), a heterogeneous region without interference of vitrification (zone B), and a heterogeneous region with partial vitrification of a polymer-rich phase (zone C) are indicated.

from 15 to 48 °C), which nearly equals the temperature of 35 °C at which c_p^{app} drops below c_p^{base} (Figure 1a, indicated by the arrow and the vertical dashed line). Note that the T_g of the homogeneous 70/30 solution equals ca. 10 °C.

The drop of c_p^{app} below its extrapolated c_p^{base}, due to a decreased contribution of mixing, can occur in the absence of (partial) vitrification as well, as is recognized for aqueous polymer systems and observed for polymers such as poly(vinyl methyl ether) (PVME)[4,43] or poly(oxypropylene) (PPO)[51] that phase separate well above their T_g. However, when partial vitrification of the PNIPAM-rich phase occurs, the drop in c_p^{app} is accentuated by an additional decrease in both c_p^{base} and c_p^{excess}. For these reasons, and supported by the quench-cooling results and the state diagram (Figure 1b), the temperature at the drop of c_p^{app} below the extrapolated experimental c_p^{base} (Figure 1, arrow and vertical dashed line) was taken as the characteristic temperature for the onset of the partial vitrification process.

Hence, three temperature regions can be introduced, as illustrated in Figure 1: a homogeneous region (zone A), a heterogeneous region without interference of vitrification (zone B), and a heterogeneous region with partial vitrification of a polymer-rich phase (zone C).

The remixing behavior upon cooling is significantly influenced by the preceding phase separation history: the temperature of demixing (zone B or C) and the annealing of the polymer/water sample above T_{demix} will determine the degree of partial vitrification, which inevitably slows down the remixing process.[36] Hence, the balance between reversing and nonreversing heat flow contributions differs upon cooling: the nonreversing heat flow is no longer negligible and amounts up to 60% of the total heat flow, depending on the sample composition. However, the sum of both heat flow contributions upon cooling, i.e., the total remixing enthalpy, is in general twice as small as the total demixing enthalpy (in absolute value), which illustrates that the remixing process is not completed upon cooling. In order to obtain complete homogeneity in zone A, water has to diffuse into the dense, vitrified PNIPAM-rich phase. The slower and incomplete remixing of the $PNIPAM_{187000}$/water system is seen in the upper curves of Figure 1a: c_p^{app} upon cooling (thin line) is smaller than upon heating (thick line). Moreover, the specific heat capacity value after cooling is about 0.1 J g^{-1} K^{-1} smaller than the initial value of the homogeneous solution in zone A, again indicating that the sample did not completely remix during cooling. After a heating/cooling cycle at 1 °C min^{-1} to 60 °C, the typical time needed to homogenize the sample at for example 20 °C (zone A) is 30 min. Such isothermal remixing, needed to obtain the equilibrium state at low temperature (zone A), is seen as an increase in c_p^{app} toward c_p^{base},[36] as was also noticed for partially miscible polymer blends with interference of vitrification during demixing[42] and for the poly(*N*-vinylcaprolactam) (PVCL)/water system.[41] The longer the solution is kept at a temperature above the onset of partial vitrification (zone C) and the higher this temperature, the higher the degree of partial vitrification of the polymer-rich phase (due to the ongoing release of water molecules, governed by the state diagram, until all mobility becomes restricted), consequently slowing down the remixing process in the homogeneous region.[36]

Note that in aqueous homopolymer systems it was found that remixing upon cooling is always slower than demixing upon heating, independent of the LCST (I, II, or III) type of demixing behavior.[8,41,43] This originates from the necessary diffusion of both components through the interfacial area, which is additionally slowed down when partial vitrification interferes during the preceding demixing step. Therefore, the difference in demixing−remixing kinetics considerably enlarges in the case of PNIPAM/water.

Similar observations hold when examining the block copolymer PNIPAM-*b*-PEO/water system (Figure 1a, middle curves), independent of the polymer concentration. This suggests that the kinetic properties are hardly influenced by the incorporated hydrophilic PEO block. Particularly, the remixing upon cooling (thin line) is again slower than the demixing upon heating (thick line). Moreover, in the homogeneous region (zone A) the value of c_p^{app} after a heat/cool cycle is lower than the initial value, indicating that the sample has not completely remixed upon cooling.

Conversely, when studying the graft-copolymers of PNIPAM and PEO (Figure 1a, lower curves), the demixing (thick line) and remixing curve (thin line) coincide for each composition,

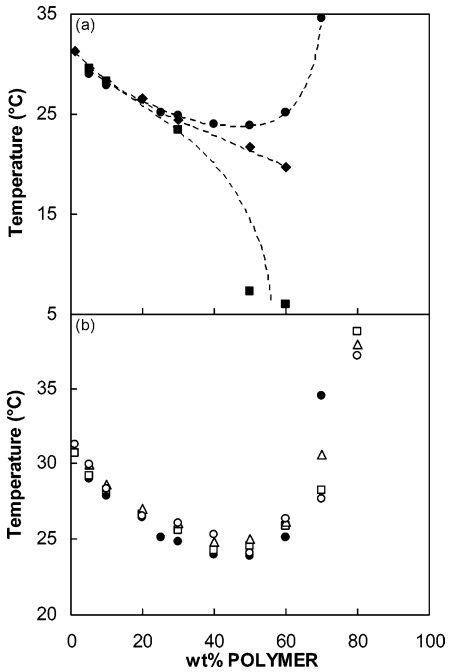

Figure 2. LCST type of demixing curves of (a) $PNIPAM_{187000}$/water (●), $PNIPAM_{180000}$-*6g*-PEO_{6000}/water (◆), and $PNIPAM_{180000}$-*10g*-PEO_{6000}/water (■); dashed lines are a guide to the eye. (b) $PNIPAM_{187000}$/water (●), $PNIPAM_{39000}$-*b*-PEO_{550}/water (Δ), $PNIPAM_{151000}$-*b*-PEO_{550}/water (□), and $PNIPAM_{345000}$-*b*-PEO_{550}/water (○).

indicating that the rate of remixing is no longer markedly slower than that of demixing, not even after partial vitrification of the polymer-rich phase (demixing in zone C). As a result, no additional time in zone A is required to completely remix the sample in contrast with aqueous solutions of either PNIPAM or PNIPAM-*b*-PEO. This implies that the introduction of hydrophilic PEO grafts is very effective for enhancing the rate of demixing and remixing, in accordance with previous observations for aqueous PVCL-*g*-PEO solutions.[41]

The introduction of a limited number (6−10) hydrophilic PEO grafts does not merely influence the kinetic properties of PNIPAM: at polymer concentrations above 50 wt % it clearly lowers the demixing temperature (Figure 2a), resulting in insolubility at room temperature. Increasing the number of PEO grafts per PNIPAM chain from 6 (Figure 2,◆) to 10 (Figure 2, ■) additionally decreases the solubility of the graft-copolymers at these high polymer concentrations. This effect is attributed to the competition between PNIPAM and PEO to interact with water, resulting in a weakening of the PNIPAM−water interactions in the vicinity of PEO.[52,53] Hence, the hydration structure surrounding the PNIPAM chains is of inferior quality, resulting in a lower demixing temperature, which becomes more important when less water molecules are available. At polymer concentrations of 30 wt % and below, thus at higher concentrations of water, this competition for water is less important, as the observed effect of the introduction of 6−10 grafts is much smaller, in fair agreement with earlier work.[44] Note that, at a concentration of about 30 wt %, increasing the number of PEO grafts to 43 and more leads to a strong increase of the solubility, indicating that with an increasing number of the PEO chains the collapse of PNIPAM is almost completely prevented.[44]

One must keep in mind that the graft-copolymers were synthesized starting from a statistical copolymer of PNIPAM and glycidyl methacrylate (GMA). The grafted and ungrafted GMA units are inherently present in the PNIPAM-*g*-PEO system and may influence the phase separation temperature as well, as has been observed for PVME-based graft-copolymers.[54]

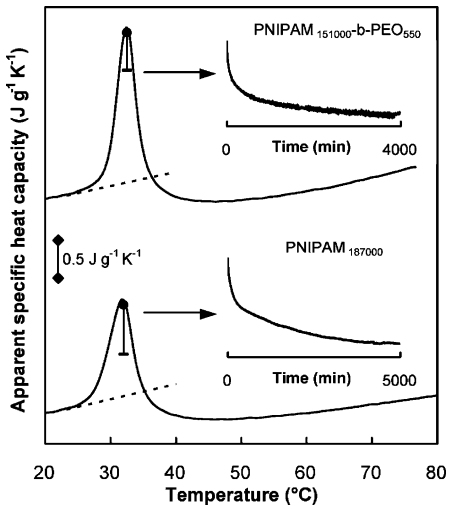

Figure 3. Overlay of the evolution in c_p^{app} for 50/50 $PNIPAM_{151000}$-*b*-PEO_{550}/water (top) and 50/50 $PNIPAM_{187000}$/water (bottom): nonisothermal demixing (continuous line); partial quasi-isothermal demixing at 32.50 °C (see inset), starting from a homogeneous solution at 10.00 °C heated at 0.2 °C min^{-1} to the respective temperature: time evolution (vertical lines, start: ●, end: −). Dashed line (extrapolated experimental c_p^{base}) is a guide to the eye. Curves are shifted vertically for clarity.

Incorporating a short hydrophilic PEO block (instead of a graft) hardly affects the demixing temperature, independent of the PNIPAM chain length, as illustrated in Figure 2b.[55] However, since the incorporation of longer PEO blocks was not investigated in this work, one must be cautious in generalizing previous observations.

2. Quasi-Isothermal Demixing of Aqueous Polymer Solutions: Phase Separation Kinetics. The kinetic properties of an aqueous polymer solution can be evaluated in more detail via quasi-isothermal MTDSC experiments,[8,36,37,41,43] which means that the underlying temperature is kept constant while the temperature modulation is maintained. After heating a $PNIPAM_{187000}$/water solution to any temperature in zone B or C (demixing), a gradual, isothermal evolution of c_p^{app} toward a final excess contribution is observed, as illustrated in Figure 3 for zone B (lower curves: inset and vertical line). This slow evolution takes up to several days and is related to a variation of the polymer/water interphase within the sample (i.e., morphology development). Note that the time needed to reach the final excess value depends on the demixing temperature; i.e., the evolution of c_p^{app} in zone C is in general even significantly slower than in zone B.[8] In some cases, however, no time dependency was noticed in zone C, indicating that the attained morphology was fixed because of the partial vitrification phenomenon. Similar quasi-isothermal demixing experiments on PNIPAM-*b*-PEO/water display an analogous behavior (Figure 3, upper curves). This suggests that the ongoing morphological changes within the phase separating sample are hardly altered by the PEO blocks. Conversely, for PEO-grafted PNIPAM, c_p^{app} is time-independent at whatever temperature within the phase separation region (zones B and C). This implies that the equilibrium excess contribution in c_p^{app} is immediately attained at each temperature (Figure 4, ○) and thus coincides with the nonisothermal demixing curve (Figure 4, continuous line), irrespective of the polymer weight fraction or the amount of PEO grafts. This again signifies that the PEO grafts promote the exchange of water at the polymer/water interphase and accelerate the diffusion of water molecules within the collapsed polymer aggregates.

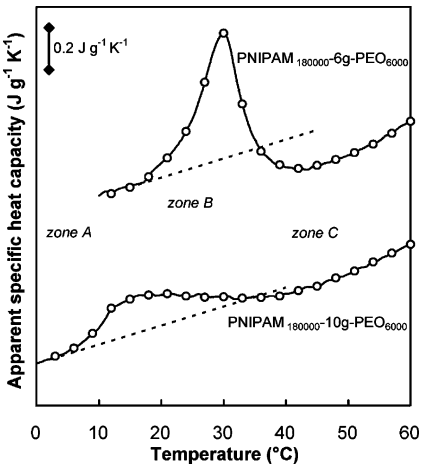

Figure 4. Overlay of the evolution in c_p^{app} for 50/50 PNIPAM$_{180000}$-*6g*-PEO$_{6000}$/water (top) and 50/50 PNIPAM$_{180000}$-*10g*-PEO$_{6000}$/water (bottom): nonisothermal demixing (continuous line) and stepwise quasi-isothermal measurements with a step of 3 °C (equilibrium value: ○). Dashed line (extrapolated experimental c_p^{base}) is a guide to the eye. Curves are shifted vertically for clarity.

Despite the similar chemical composition of the PNIPAM−PEO block and graft copolymers studied, their aqueous solutions display a totally different thermoresponsive behavior. The nonisothermal and quasi-isothermal results strongly suggest that the enhanced demixing and remixing kinetics are not necessarily caused by the introduction of a hydrophilic component as such (i.e., PEO) but that the molecular architecture is also important (graft vs block). Therefore, the attained morphology after phase separation must be dissimilar for the block and graft copolymers studied. In the case of PNIPAM-*g*-PEO, it is thought that the hydrophilic PEO chains become trapped inside the vitrified PNIPAM aggregate (Figure 5), by which they are able to improve the diffusion rate of water molecules and as such the demixing and remixing kinetics. For the block copolymers, the PEO chains are thought to be situated mainly at the polymer−water interface of the vitrified PNIPAM aggregates (Figure 5). In this position, the PEO blocks do not enhance the transport of water molecules inside the vitrified PNIPAM aggregate. This seems plausible, since in the case of block copolymers, the (short) PEO chains can rearrange more easily at the aggregate surface. The formation of such a core−shell structure will of course become more difficult as the length of the PEO blocks increases (not investigated in this work). The longer the PEO chain length, the higher the probability that it becomes trapped inside the vitrified PNIPAM aggregate. In that case, the morphology after phase separation from the aqueous solution will be close to the one suggested for the graft-copolymers.

One must note that in dilute aqueous solutions amphiphilic copolymers of PEO and PNIPAM have been reported to form a core−shell structure above the phase separation temperature of PNIPAM, irrespective of the molecular architecture.[44,45,55−63] These observations suggest the thermoresponsive behavior of block and graft copolymers to be quite similar, which is in contrast to the reasoning described above and illustrated in Figure 5. For that reason the phase separation behavior of dilute 1/99 polymer/water solutions of PNIPAM$_{187000}$/water, PNIPAM$_{151000}$-*b*-PEO$_{550}$/water, and PNIPAM$_{180000}$-*6g*-PEO$_{6000}$/water, respectively, was investigated. Figure 6 (on the left) illustrates that when performing a partial quasi-isothermal demixing experiment in zone B, c_p^{app} is time-dependent, even for the grafted PNIPAM system. It indeed confirms the assumption that in dilute conditions graft or block copolymers attain a comparable phase-separated morphology, which most likely is a core−shell structure (Figure 6, on the right). In this case, even for the graft copolymer, the PEO chains experience few restrictions to rearrange at the surface of the aggregates. Accordingly, the suggested morphologies from Figure 5 are only valid at polymer concentrations well above the critical overlap concentration with restrictions of entangled polymer coils.

Finally, the better the distribution of the PEO chains trapped inside the copolymer aggregate, the more easily they can enhance the transport of water molecules to obtain an optimum response behavior. Therefore, the miscibility of the thermoresponsive PNIPAM backbone and the hydrophilic PEO chains seems essential too, since it will alter the attained morphology in the PNIPAM aggregate. In the case of miscibility, the entrapped PEO chains will be homogeneously distributed (Figure 5), whereas immiscibility will result in domain formation (i.e., polymer−polymer phase separation) inside the vitrified polymer aggregate (Figure 5).

B. Miscibility of the Copolymer Constituents: PNIPAM/PEO Blends. Examining the potential miscibility of the copolymer constituents (i.e., the binary PNIPAM/PEO blend) might provide more insight into the thermoresponsive properties of the corresponding copolymers in water (see previous section).

Evaluation of T_g for Monitoring Liquid−Liquid Demixing in PNIPAM/PEO Blends. All PNIPAM$_{187000}$/PEO$_{300}$ blends are transparent at room temperature, and they remain transparent upon heating up to 150 °C as observed by optical microscopy, thus suggesting miscibility within the entire composition range up to 150 °C. If so, one would expect each (homogeneous) polymer blend to have a single glass transition temperature.[64,65] Figure 7 shows an overlay of c_p upon cooling for blends of different composition. Those blends containing less than 40 wt % or more than 87 wt % of PNIPAM can indeed be described by a single, composition-dependent T_g, seen as a stepwise decrease in c_p upon cooling. However, for blends with an amount of PNIPAM between 40 and 87 wt %, a second T_g is noticeable. Therefore, one can conclude that the PNIPAM$_{187000}$/PEO$_{300}$ blend system displays a miscibility gap at intermediate blend compositions, represented by two glass transitions. These MTDSC results illustrate that optical microscopy is insufficient to unambiguously analyze the miscibility behavior of this type of blend. Similar observations were made for poly(*N*-vinylpyrrolidone) (PVP)/PEO blends, for which the multiple T_g's were ascribed to the existence of an intermolecular physical network in equilibrium with a homogeneous binary polymer phase.[66−68]

In order to exclude any possible influence of the blend preparation procedure, a blend that exhibits two T_g's (i.e., 60/40 PNIPAM$_{187000}$/PEO$_{300}$) was prepared using five different solvents: chloroform, dichloromethane, *N*,*N*-dimethylformamide, methanol, and tetrahydrofuran. This, however, had no effect on the observed glass transitions and thus on the miscibility. As some of the heterogeneous samples are partially vitrified at room temperature, which might kinetically hinder the mixing process during storage, they were annealed at different temperatures. Again, no difference could be noticed, meaning that no additional mixing took place at more elevated annealing temperatures. Finally, in stepwise quasi-isothermal cooling experiments in the heterogeneous glass transition region, no time dependence was noticed, and the quasi-isothermally measured c_p values coincide with the normal cooling curves of Figure 7.

This study of the PNIPAM$_{187000}$/PEO$_{300}$ blend indicates that the appearance and the positioning of the observed glass transition(s) are inherent to the blend composition and independent of the annealing temperature and/or time. As no

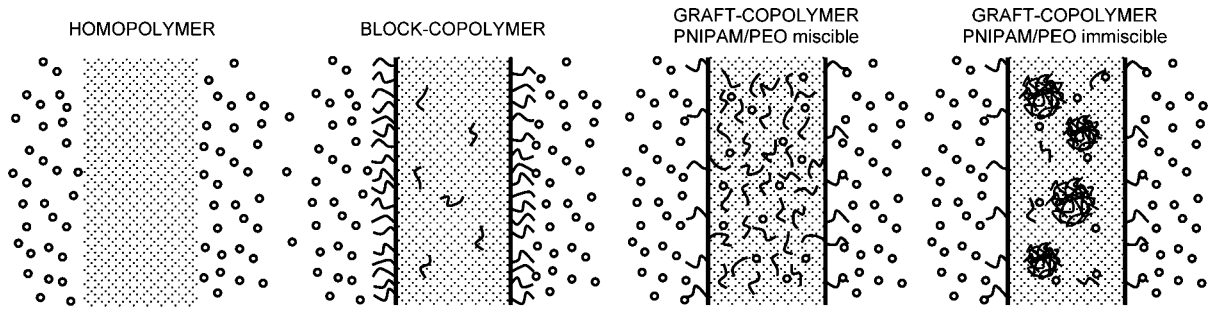

Figure 5. Schematic presentation of the attained morphology in water above T_{demix} for the PNIPAM homopolymer and block and graft copolymers (PEO and thermoresponsive PNIPAM aggregate miscible or immiscible). Shaded area: thermoresponsive PNIPAM aggregate; black lines: PEO; and ○: water molecules.

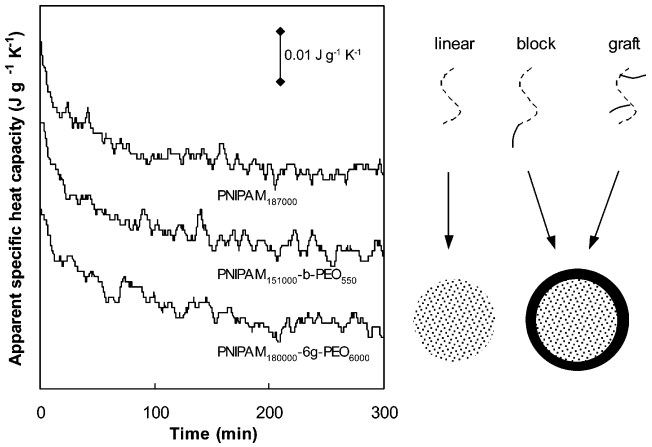

Figure 6. Left: c_p^{app} during partial quasi-isothermal demixing at 32.01 °C of 1/99 $PNIPAM_{187000}$/water, $PNIPAM_{151000}$-*b*-PEO_{550}/water, and $PNIPAM_{180000}$-*6g*-PEO_{6000}/water, starting from a homogeneous solution at 10.00 °C heated at 0.2 °C min^{-1} to the respective temperature. Right: schematic representation of the attained morphology in water above T_{demix}. Dashed lines/shaded area: PNIPAM; black lines/area: PEO.

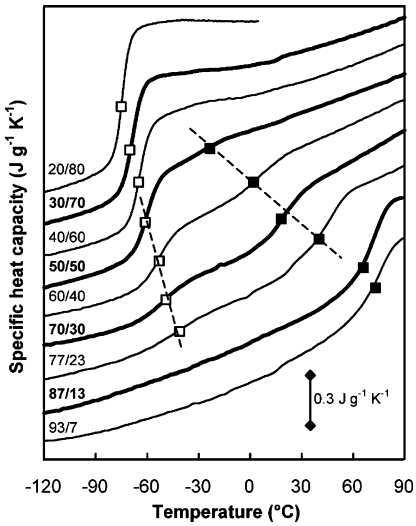

Figure 7. c_p during nonisothermal cooling of different $PNIPAM_{187000}$/PEO_{300} compositions: □, T_g PEO-rich phase; ■, T_g PNIPAM-rich phase. Curves are shifted vertically for clarity.

demixing or remixing transformations are observed, nothing can be concluded regarding the LCST or UCST type of demixing behavior. Nevertheless, the change of T_g with the blend composition allows locating the miscibility gap of this system, as summarized in Figure 8.

Figure 9 illustrates the evolution of c_p^{app} upon heating for several $PNIPAM_{187000}$/PEO_{1000} compositions. The $PNIPAM_{187000}$/PEO_{1000} system approaches the configuration of the graft copolymers of interest. In this case, the melting of PEO is always observed (near 45 °C), followed by devitrification of a PNIPAM-rich phase. The ability of PEO to crystallize at any PNIPAM concentration again indicates their limited miscibility. However, the observed T_g (at ca. 110 °C) is still lower than the glass transition temperature of pure PNIPAM (i.e., 140 °C), suggesting a certain degree of mixing. The miscibility gap at intermediate blend composition is substantially enlarged in comparison with the $PNIPAM_{187000}$/PEO_{300} system, as can be seen in Figure 10.

For blends with PEO_{2000} (not shown), the T_g of pure PNIPAM is always observed, independently of the thermal history. The reduced miscibility for higher molar masses of PEO could be due to the lower concentration of PEO terminal groups that

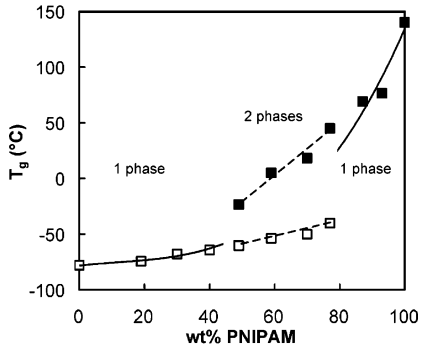

Figure 8. State diagram of $PNIPAM_{187000}$/PEO_{300}: T_g−composition data (see Figure 7). Dashed lines indicate T_g within the two-phase region, whereas the continuous lines denote the composition dependence of T_g for the homogeneous blends.

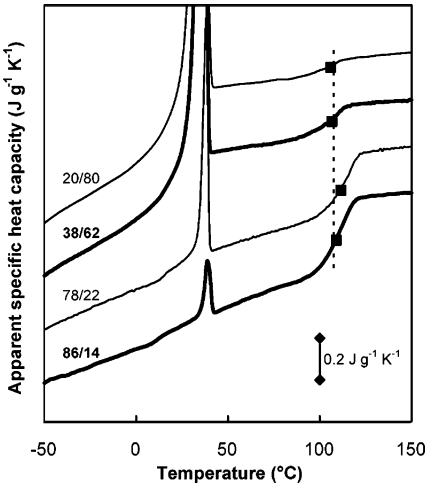

Figure 9. c_p^{app} during nonisothermal heating of different $PNIPAM_{187000}$/PEO_{1000} compositions: ■, T_g PNIPAM-rich phase. Curves are shifted vertically for clarity.

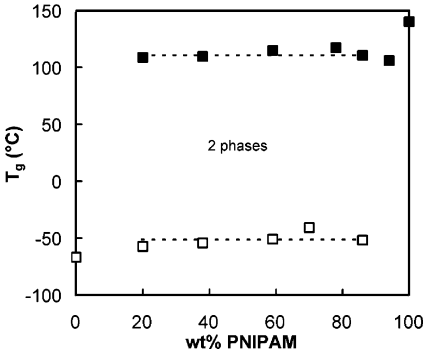

Figure 10. State diagram of $PNIPAM_{187000}/PEO_{1000}$: T_g−composition data (see Figure 9). Dashed lines indicate T_g within the two-phase region.

possibly provide the intermolecular specific interactions required for the (partial) miscibility with PNIPAM, as was observed for the lower molar mass PEO's.[66−68]

These studies on PNIPAM/PEO blends illustrate that short PEO chains have a tendency to be at least partially miscible with PNIPAM. Moreover, copolymerization additionally improves the constituents' miscibility. Therefore, one can expect the PEO grafts to be fairly homogeneously distributed within the PNIPAM aggregates formed during phase separation in the aqueous solution. Moreover, as the polymer aggregates vitrify, the PEO grafts are immobilized within (see also Figure 5). This morphology should optimize the transport of water within the thermoresponsive system, giving rise to a fast thermal response rate.

Conclusions

As has been demonstrated, the phase behavior of PEO-modified thermoresponsive PNIPAM copolymers in water is affected by the macromolecular architecture. The PNIPAM-*b*-PEO/water solutions reveal thermoresponsive properties similar to the binary PNIPAM/water system. The demixing temperatures and the transformation kinetics are hardly influenced. In both cases, the remixing of the aqueous polymer system is substantially slower than the preceding demixing. In contrast, aqueous solutions of PNIPAM-*g*-PEO show a decrease in demixing temperature when incorporating 6−10 grafts of PEO, especially at low water content (i.e., at a polymer concentration of 50 wt % or more). Furthermore, the thermal response of the aqueous PNIPAM-*g*-PEO system is significantly faster than in the case of either pure PNIPAM or PNIPAM-*b*-PEO. The influence of the macromolecular architecture on the thermal response rate is not observed for dilute solutions. These findings have been interpreted in terms of the partial miscibility of PNIPAM and PEO, and possible morphologies of the phase-separated polymer aggregates have been suggested. Similar observations have previously been reported for systems based on PVCL.[41]

Partial vitrification of the thermoresponsive polymer is an additional factor that affects the demixing and remixing rate of the aqueous polymer systems studied. As the PNIPAM-rich phase can vitrify above the demixing temperature, the mobility of incorporated PEO grafts is restricted. Hence, these grafts remain within the vitrified polymer aggregate and enhance the transport of water molecules.

In conclusion, the copolymer concentration, the macromolecular architecture, (partial) miscibility of the copolymer components, and (partial) vitrification of the thermoresponsive component are important parameters for an accelerated thermal response rate of aqueous solutions of amphiphilic copolymers containing PNIPAM and PEO. This concept is applicable to other analogues amphiphilic copolymer systems.

Acknowledgment. Kurt Van Durme thanks the Institute for the Promotion of Innovation through Science and Technology in Flanders (IWT) for a PhD grant. Guy Van Assche is a Postdoctoral Fellow of the Research Foundation-Flanders (FWO-Vlaanderen). This work was supported by a grant from the Research Foundation-Flanders (FWO-Vlaanderen).

References and Notes

(1) Snowden, M.; Murray, M.; Chowdry, B. Z. *Chem. Ind.* **1996**, *14*, 531−534.
(2) Aseyev, V.; Tenhu, H.; Winnik, F. *Adv. Polym. Sci.* **2006**, *196*, 1−85.
(3) Šolc, K.; Dušek, K.; Koningsveld, R.; Berghmans, H. *Collect. Czech. Chem. Commun.* **1995**, *60*, 1661−1688.
(4) Schäfer-Soenen, H.; Moerkerke, R.; Berghmans, H.; Koningsveld, R.; Dušek, K.; Šolc, K. *Macromolecules* **1997**, *30*, 410−416.
(5) Moerkerke, R.; Meeussen, F.; Koningsveld, R.; Berghmans, H. *Macromolecules* **1998**, *31*, 2223−2229.
(6) Afroze, F.; Nies, E.; Berghmans, H. *J. Mol. Struct.* **2000**, *554*, 55−68.
(7) Meeussen, F.; Nies, E.; Verbrugghe, S.; Goethals, E.; Du Prez, F.; Berghmans, H. *Polymer* **2000**, *41*, 8597−8602.
(8) Van Durme, K.; Loos, W.; Du Prez, F. E.; Van Mele, B. *Polymer* **2005**, *46*, 9851−9862.
(9) Osada, Y.; Kishi, R.; Hasebe, M. *J. Polym. Sci., Part C: Polym. Lett.* **1987**, *25*, 481−485.
(10) Shinohara, S.; Tajima, N.; Yanagisawa, K. *J. Intell. Mater. Syst. Struct.* **1996**, *7*, 254−259.
(11) Liu, Z.; Calvert, P. *Adv. Mater.* **2000**, *12*, 288−291.
(12) Gotoh, T.; Okamoto, H.; Sakohara, S. *J. Chem. Eng. Jpn.* **2004**, *37*, 347−352.
(13) Rao, K. V. R.; Devi, K. P. *Int. J. Pharm.* **1988**, *48*, 1−13.
(14) Brazel, C. S.; Peppas, N. A. *Polym. Mater. Sci. Eng.* **1996**, *74*, 370−371.
(15) Qiu, Y.; Park, K. *Adv. Drug Delivery Rev.* **2001**, *53*, 321−339.
(16) Gupta, P.; Vermani, K.; Garg, S. *Drugs Discov. Today* **2002**, *7*, 569−579.
(17) Kikuchi, A.; Okano, T. *Macromol. Symp.* **2004**, *205*, 217−227.
(18) Liang, L.; Rieke, P. C.; Liu, J.; Fryxell, G. E.; Young, J. S.; Engelhard, M. H.; Alford, K. L. *Langmuir* **2000**, *16*, 8016−8023.
(19) Choi, Y. J.; Yamaguchi, T.; Nakao, S. I. *Ind. Eng. Chem. Res.* **2000**, *39*, 2491−2495.
(20) Akashi, R.; Tsutsui, H.; Komura, R. *Adv. Mater.* **2002**, *14*, 1808−1811.
(21) Asher, S. A.; Weismann, J. M.; Sunkara, H. B. US Patent 6165389, 2000.
(22) Kanazawa, R.; Yoshida, T.; Gotoh, T.; Sakohara, S. *J. Chem. Eng. Jpn.* **2004**, *37*, 59−66.
(23) Miyata, T.; Uragami, T.; Nakamae, K. *Adv. Drug Delivery Rev.* **2002**, *54*, 79−98.
(24) Scarpa, J. S.; Müller, D. D.; Klotz, I. M. *J. Am. Chem. Soc.* **1967**, *89*, 6024−6030.
(25) Heskins, M.; Guillet, J. E. *J. Macromol. Sci., Chem.* **1968**, *2*, 1441−1455.
(26) Yamamoto, I.; Iwasaki, K.; Hirotsu, S. *J. Phys. Soc. Jpn.* **1989**, *58*, 210−215.
(27) Wang, X.; Qiu, X.; Wu, C. *Macromolecules* **1998**, *31*, 2972−2976.
(28) Gorelov, A. V.; Du Chesne, A.; Dawson, K. A. *Physica A* **1997**, *240*, 443−452.
(29) Aseyev, V.; Hietala, S.; Laukkanen, A.; Nuopponen, M.; Confortini, O.; Du Prez, F. E.; Tenhu, H. *Polymer* **2005**, *46*, 7118−7131.
(30) Schild, H. G. *Prog. Polym. Sci.* **1992**, *17*, 163−249.
(31) Lin, S. Y.; Chen, K. S.; Run-Chu, L. *Polymer* **1999**, *40*, 2619−2624.
(32) Ramon, O.; Kesselman, E.; Berkovici, R.; Cohen, Y.; Paz, Y. *J. Polym. Sci., Part B: Polym. Phys.* **2001**, *39*, 1665−1677.
(33) Ohta, H.; Ando, I.; Fujishige, S.; Kubota, K. *J. Polym. Sci., Part B: Polym. Phys.* **1991**, *29*, 963−968.
(34) Shibayama, M.; Suetoh, Y.; Nomura, S. *Macromolecules* **1996**, *29*, 6966−6968.
(35) Boutris, C.; Chatzi, E. G.; Kiparissides, C. *Polymer* **1997**, *38*, 2567−2570.
(36) Van Durme, K.; Van Assche, G.; Van Mele, B. *Macromolecules* **2004**, *37*, 9596−9605.
(37) Van Durme, K.; Delellio, L.; Kudryashov, E.; Buckin, V.; Van Mele, B. *J. Polym. Sci., Part B: Polym. Phys.* **2005**, *43*, 1283−1295.
(38) Cheng, H.; Shen, L.; Wu, C. *Macromolecules* **2006**, *39*, 2325−2329.
(39) Zhang, X.; Chu, C. *J. Mater. Chem.* **2003**, *13*, 2457−2464.

(40) Kaneko, Y.; Nakamura, S.; Sakai, K.; Aoyagi, T.; Kikuchi, A.; Sakurai, Y.; Okano, T. *Macromolecules* **1998**, *31*, 6099−6105.
(41) Van Durme, K.; Verbrugghe, S.; Du Prez, F. E.; Van Mele, B. *Macromolecules* **2004**, *37*, 1054−1061.
(42) Swier, S.; Pieters, R.; Van Mele, B. *Polymer* **2002**, *43*, 3611−3620.
(43) Swier, S.; Van Durme, K.; Van Mele, B. *J. Polym. Sci., Part B: Polym. Phys.* **2003**, *41*, 1824−1836.
(44) Virtanen, J.; Baron, C.; Tenhu, H. *Macromolecules* **2000**, *33*, 336−341.
(45) Virtanen, J.; Holappa, S.; Lemmetyinen, H.; Tenhu, H. *Macromolecules* **2002**, *35*, 4763−4769.
(46) Virtanen, J.; Tenhu, H. *Macromolecules* **2000**, *33*, 5970−5975.
(47) Ganachaud, F.; Monterio, M. J.; Gilbert, R. G.; Dourges, M. A.; Thang, S. H.; Rizzardo, E. *Macromolecules* **2000**, *33*, 6738−6745.
(48) Wunderlich, B.; Jin, Y.; Boller, A. *Thermochim. Acta* **1994**, *238*, 277−293.
(49) Reading, M.; Luget, A.; Wilson, R. *Thermochim. Acta* **1994**, *238*, 295−307.
(50) *Modulated-Temperature Differential Scanning Calorimetry: Theoretical and Practical Applications in Polymer Characterisation (Hot Topics in Thermal Analysis and Calorimetry)*; Reading, M., Hourston, D. J., Eds.; Springer: London, UK, 2006.
(51) Batsberg, W.; Ndoni, S.; Trandum, C.; Hvidt, S. *Macromolecules* **2004**, *37*, 2965−2971.
(52) Yanul, N. A.; Kirsh, Y. E.; Verbrugghe, S.; Goethals, E. J.; Du Prez, F. E. *Macromol. Chem. Phys.* **2001**, *201*, 1700−1709.
(53) Verbrugghe, S.; Bernaerts, K.; Du Prez, F. E. *Macromol. Chem. Phys.* **2003**, *204*, 1217−1225.
(54) Confortini, O.; Van Durme, K.; El Ouaamari, I.; Van Mele, B.; Du Prez, F. E. *Polymer*, in press.
(55) Cao, W. X.; Zhang, T. *Chem. Res. Chin. Univ.* **1997**, *13*, 157−162.
(56) Lee, K. K.; Jung, J. C.; Jhon, M. S. *Polym. Bull. (Berlin)* **1998**, *40*, 455−460.
(57) Virtanen, J.; Lemmetyinen, H.; Tenhu, H. *Polymer* **2001**, *42*, 9487−9493.
(58) Lin, H. H.; Cheng, Y. L. *Macromolecules* **2001**, *34*, 3710−3715.
(59) Berlinova, I. V.; Dimitrov, I. V.; Vladimirov, N. G.; Samichkov, V.; Ivanov, Y. *Polymer* **2001**, *42*, 5963−5971.
(60) Rackaitis, M.; Stawhecker, K.; Manias, E. *J. Polym. Sci., Part B: Polym. Phys.* **2002**, *40*, 2339−2342.
(61) Verbrugghe, S.; Laukkanen, A.; Aseyev, V.; Tenhu, H.; Winnik, F. M.; Du Prez, F. E. *Polymer* **2003**, *44*, 6807−6814.
(62) Kjøniksen, A. L.; Nyström, B.; Tenhu, H. *Colloids Surf., A* **2003**, *228*, 75−83.
(63) Zhu, P. W. *J. Mater. Sci.: Mater. Med.* **2004**, *15*, 567−573.
(64) Chiu, S. C.; Kwei, T. K.; Pearce, E. M. *J. Therm. Anal. Calorim.* **2000**, *59*, 71−81.
(65) Pellerin, C.; Prud'homme, R. E.; Pezolet, M. *Polymer* **2003**, *44*, 3291−3297.
(66) Feldstein, M. M.; Shandryuk, G. A.; Kuptsov, S. A.; Platé, N. A. *Polymer* **2000**, *41*, 5327−5338.
(67) Feldstein, M. M.; Kuptsov, S. A.; Shandryuk, G. A. *Polymer* **2000**, *41*, 5339−5348.
(68) Feldstein, M. M.; Kuptsov, S. A.; Shandryuk, G. A.; Platé, N. A. *Polymer* **2001**, *42*, 981−990.

MA062538G